Supporting Information

# Single-Atom Co-$N_4$ Electrocatalyst Enabling Four-Electron Oxygen Reduction with Enhanced Hydrogen Peroxide Tolerance for Selective Sensing

Fei Wu,[1,2,†] Cong Pan,[1,2,†] Chun-Ting He,[3,†] Yunhu Han,[4] Wenjie Ma,[1,2] Huan Wei,[1,2] Wenliang Ji,[1] Wenxing Chen,[5] Junjie Mao,[6] Ping Yu,[1,2] Dingsheng Wang,[4] Lanqun Mao[1,2,*] Yadong Li [4,*]

[1] *Beijing National Laboratory for Molecular Sciences, Key Laboratory of Analytical Chemistry for Living Biosystems, Institute of Chemistry, The Chinese Academy of Sciences (CAS), Beijing 100190, China*

[2] *University of Chinese Academies of Sciences, Beijing 100049, China.*

[3] *MOE Key Laboratory of Functional Small Organic Molecule, College of Chemistry and Chemical Engineering, Jiangxi Normal University, Nanchang 330022, China.*

[4] *Department of Chemistry, Tsinghua University, Beijing 100084, China.*

[5] *Beijing Key Laboratory of Construction Tailorable Advanced Functional Materials and Green Applications, School of Materials Science and Engineering, Beijing Institute of Technology, Beijing, 100081, China.*

[6] *College of Chemistry and Materials Science, Anhui Normal University, Wuhu 241002, China.*

[†] These authors contributed equally: F. Wu, C. Pan, and C.-T. He

[*] Correspondence to: lqmao@iccas.ac.cn, ydli@tsinghua.edu.cn

## Table of Contents

# 1. Experimental Section

## 1.1 Reagents and materials

Nafion® D-521 dispersion (5% w/w in water and 1-propanol), *N, N*-dimethylformamide (DMF) and tetraethoxysilane (TEOS) were purchased from Alfa Aesar. Cobalt (II) acetate tetrahydrate ($Co(oAc)_2 \cdot 4H_2O$) was obtained from Sinopharm Chemical. 5, 10, 15, 20-Tetra(4-(imidazol-1-yl) phenyl) porphyrindine (TIPP) was purchased from Shanghai Chemical Reagents, China. Phosphate buffer mimicking *in vivo* fluid was prepared by mixing NaCl (126 mM), KCl (2.4 mM), $KH_2PO_4$ (0.5 mM), $MgCl_2$ (0.85 mM), $NaHCO_3$ (27.5 mM), $Na_2SO_4$ (0.5 mM), and $CaCl_2$ (1.1 mM) in deionized water and the solution pH was adjusted to pH 7.4. All chemicals were of analytical grade and used without further purification. All aqueous solutions were prepared with Milli-Q water. Unless specifically stated, all experiments were carried out at room temperature.

## 1.2 Synthesis of Co-$N_4$/C and HNCS catalysts

Silica spheres were synthesized by the TEOS's condensation and ammonia-catalyzed hydrolysis in an aqueous ethanol according to the classical Stöber method.[1,2] Briefly, 0.6 mL of TEOS was quickly injected into a stirred mixture of deionized water (5 mL), absolute ethanol (15 mL), and 28% $NH_3 \cdot H_2O$ (0.7 mL). After continuous stirring for 10 h, precipitates were collected by centrifugation, washed with ethanol for three times and dried.

To prepare Co-TIPP, $Co(OAc)_2 \cdot 4H_2O$ (150 mg) and TIPP (175 mg) were dissolved in 100 mL DMF, and the solution was heated to reflux at 175 °C for 3 h. As the excess solvent was evaporated to give a final volume of 20 mL, the solution left was cooled down to room temperature, added into 200 mL frozen deionized water, and let stand for 1 h. Formed precipitates were collected by centrifugation, washed with deionized water for several times and dried in vacuum at 120 °C for 4 h.

Co-$N_4$/C catalyst was synthesized as reported previously.[3] In brief, a mixture of Co-TIPP (20 mg, 0.02 mmol), TIPP (280 mg, 0.32 mmol) and $SiO_2$ (500 mg) in 100 mL DMF was prepared in a 250 mL round-bottom flask. After injection of α,α'-dibromo-p-xylene (179.5 mg, 0.68 mmol) dissolved in 20 ml DMF, the mixture was heated at 110 °C under stirring for 24 h. The product was collected by centrifugation, washed by DMF and ethanol, and dried at 80 °C under vacuum for 12 h. Resulting powder ($SiO_2$@Co-TIPP/TIPP-polymer) was collected into a tube furnace and gradually heated to 800 °C in 3 h (5 °C $min^{-1}$) under $H_2$/Ar (5:95) gas flow.

Then the powder was cooled to room temperature and etched by 6 M NaOH aqueous solution at 60 °C for 24 h to remove the $SiO_2$ template. The final product was centrifuged, washed by water and ethanol, and dried at 30 °C in vacuum overnight. HNCS catalyst was synthesized using the same procedure with more TIPP (300 mg, 0.34 mmol) in the absence of Co-TIPP.

### 1.3 Structural characterizations

Scanning electron microscope (SEM) images were obtained with a Hitachi S4800 scanning electron microscope. HAADF-STEM images were obtained with a JEOL-2100F FETEM (electron acceleration energy set at 200 kV). Elemental analysis of Co in the solid samples was carried out by an Optima 7300 DV inductively coupled plasma atomic emission spectrometer (ICP-AES). XAFS spectra at the Co K-edge (7709 eV) were collected with the beamline 1W1B station of the Beijing Synchrotron Radiation Facility, China. Co K-edge XANES was conducted in a fluorescence mode. The spectra of Co foil and CoPc were recorded as references. All experiments were conducted in ambient conditions. The obtained EXAFS data were processed according to the standard procedure employing the ATHENA module inside the *IFEFFIT* software packages. The $k_3$-weighted EXAFS spectra were acquired by subtracting the post-edge background from the full absorption spectrum and then normalizing with respect to the edge-jump step. Subsequently, $k^3$-weighted $x$(k) data of Co K-edge were Fourier transformed to real (R) space. Hanning window was used ($d_K$ = 1.0 $Å^{-1}$) to resolve the EXAFS contributions from different coordination shells.

The acquired EXAFS data were processed according to the standard procedures using the ATHENA module implemented in the *IFEFFIT* software packages. The $k^3$-weighted EXAFS spectra were obtained by subtracting the post-edge background from the overall absorption spectrum and then normalizing with respect to the edge-jump step. Subsequently, $k^3$-weighted $x$(k) data of Co K-edge were Fourier transformed to real (R) space using Hanning windows (dk = 1.0 $Å^{-1}$) to resolve the EXAFS contributions from different coordination shells. To obtain the quantitative structural parameters around central atoms, least-squares fitting is performed using the ARTEMIS module of IFEFFIT software packages. The following EXAFS equation was used:

$$\chi(k) = \sum_j \frac{N_j S_0^2 F_j(k)}{kR_j^2} \exp[-2k^2\sigma_j^2] \exp[\frac{-2R_j}{\lambda(k)}] \sin[2kR_j + \phi_j(k)] \qquad \text{S1}$$

$S_0^2$ is the amplitude reduction factor; $F_j(k)$ is the effective curved-wave backscattering amplitude; $N_j$ is the

number of neighbors in the $j^{th}$ atomic shell; $R_j$ is the distance between the X-ray absorbing central atom and the atoms in the $j^{th}$ atomic shell (backscatterer); $\lambda$ is the mean free path in Å, $\phi_j(k)$ is the phase shift (including the phase shift for each shell and the total central atom phase shift); and $\sigma_j$ is the Debye-Waller parameter of the $j^{th}$ atomic shell (variation of distances around the average $R_j$). The functions $F_j(k)$, $\lambda$ and $\phi_j(k)$ are calculated with the ab initio code FEFF8.2.

### 1.4 Preparation of platinized glassy carbon electrodes (Pt-GCEs)

Pt-GCEs were prepared by electrochemical deposition of Pt nanoparticles onto the glassy carbon electrodes in the solution of 0.5 M $H_2SO_4$ containing 1.0 mM $H_2PtCl_6$, with cyclic voltammetry from +0.5 V to -0.7 V for continuous 50 cycles at a scan rate of 100 $mV \cdot s^{-1}$. The Pt-GCEs were rinsed with deionized water and dried at room temperature.

### 1.5 Microelectrode modification

Carbon fiber electrodes (CFEs, 7 μm in diameter) were prepared as reported previously.[4] The CFEs were modified with a hydrophobic monolayer by continuously cycling the electrodes within a potential window between -0.2 V and +1.4 V (*vs*. Ag/AgCl) for 50 cycles at a scan rate of 10 $mV \cdot s^{-1}$ in ethanol containing 10 μM hexylamine and 2 mM $LiClO_4$. After surface modification, the CFEs were rinsed with deionized water and ethanol for three times, and placed in pure water for 30 minutes to stabilize the layer before use.

To confine Co-$N_4$/C nanospheres on to CFEs, the hydrophobically modified CFEs were immersed in an aqueous dispersion of Co-$N_4$/C (1 $mg \cdot mL^{-1}$) for 12 h. After that, the CFEs were taken out of the dispersion and washed with deionized water and dried at room temperature.

Platinized-CFEs were prepared by electrochemical deposition of Pt nanoparticles onto bare CFEs from the solution of 0.5 M $H_2SO_4$ containing 1.0 mM $H_2PtCl_6$ with cyclic voltammetry from +0.5 V to -0.7 V for continuous 50 cycles at a scan rate of 10 $mV \cdot s^{-1}$. The Pt-CFEs were rinsed with deionized water and dried at room temperature.

### 1.6 Electrochemical measurements

Electrochemical measurements were carried out in a three-electrode system in phosphate-buffered electrolyte (pH 7.4) on a CHI 730D electrochemical workstation (Shanghai Chenhua Instruments, China). GCEs and CFEs were used as working electrodes, a platinum wire as counter electrode and Ag/AgCl electrode as

reference electrode.

For hydrodynamic measurements, a Co-$N_4$/C-coated E6R2 Fixed-Disk glassy carbon RRDE (disk OD = 5.61 mm, ring OD = 7.92 mm, PINE Instruments, USA) was used as working electrode controlled by WaveDriver® 200 Integrated Bipotentiostat (PINE instruments, USA). Linear sweep voltamograms were collected at various rotating speeds from 400 to 2000 rpm with a scan rate of 10 mV·$s^{-1}$ in $O_2$-saturated phosphate buffer (pH 7.4). For kinetic analysis by RDE measurements, electron transfer number ($n$) and current density ($J_k$) were calculated from the Koutecky-Levich equation:

$$\frac{1}{J} = \frac{1}{J_L} + \frac{1}{J_k} = \frac{1}{B\omega^{\frac{1}{2}}} + \frac{1}{J_k} \quad \text{S2}$$

$$B = 0.62nFc_O D_O^{\frac{2}{3}} v^{-\frac{1}{6}} \quad \text{S3}$$

$J$ is the measured current density; $J_K$ and $J_L$ respectively represent the kinetic and diffusion-limiting current densities; $\omega$ is the angular velocity; n is the overall electron transfer number in $O_2$ reduction; $F$ is the Faraday constant ($F$= 96,485 C·$mol^{-1}$); $c_o$ is the bulk concentration of $O_2$ ($c_o$= 1.2 × $10^{-3}$ mol·$cm^{-3}$); $D_O$ is the diffusion coefficient of $O_2$ in aqueous solution at 20 °C (1.9 × $10^5$ $cm^2$·$s^{-1}$); and $v$ is the kinematic viscosity of the electrolyte solution (0.01 $cm^2$·$s^{-1}$).

For kinetic analysis by RRDE measurements, the potential applied to disk electrode was scanned cathodically at a scan rate of 10 mV·$s^{-1}$ and the potential of ring electrode was set to +0.50 V *vs*. Ag/AgCl in oxygen-saturated phosphate buffer (pH 7.4). Electron transfer number ($n$) was calculated from following equation:

$$n = 4 \times \frac{I_d}{I_d + \frac{I_r}{N}} \quad \text{S4}$$

$I_d$ is the disk current; $I_r$ is the ring current; and $N$ = 0.37 is the current collection efficiency of the Pt ring on the RRDE electrode.

### 1.7 Calculation of rate constants for ORR by Damjanovic modeling

The RRDE voltammetric equations were derived by Damjanovic *at el.*[5] to calculate the rate constants ($k_1$, $k_2$ and $k_3$) of the ORR model shown in **Scheme 1** and expressed as follows:

**Scheme 1.** Damjanovic model of ORR.

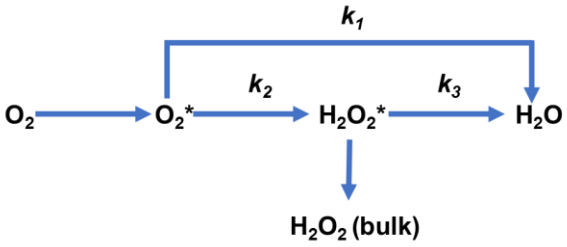


$$\frac{I_d}{I_r} = \frac{1+2k_1/k_2}{N} + \frac{2(1+k_1/k_2)}{NZ_2} k_3 \omega^{-1/2} \quad \text{S5}$$

$$\frac{I_{dl}}{I_{dl}-I_d} = 1 + \frac{k_1+k_2}{Z_1} \omega^{-1/2} \quad \text{S6}$$

where $Z_1 = 0.2D_{O_2}^{2/3} v^{-1/6}$ and $Z_2 = 0.2D_{H_2O_2}^{2/3} v^{-1/6}$; $I_d$ is the disk current; $I_r$ is the ring current; $I_{dl}$ is the disk limiting current; ω is the rotational speed of electrode; $N$ is the collection efficiency; $D_{H_2O_2}$ and $D_{O_2}$ are the respective diffusion coefficients of $H_2O_2$ and $O_2$; and $v$ is the kinematic viscosity of the solution used. By combining the intercepts and slopes of both $I_d/I_r$ *vs.* $\omega^{-1/2}$ and $I_{dl}/(I_{dl}-I_d)$ *vs.* $\omega^{-1/2}$ plots, the step rate constants can be expressed by following equations:

$$k_1 = S_2 Z_1 \frac{I_1 N - 1}{I_1 N + 1} \quad \text{S7}$$

$$k_2 = \frac{2Z_1 S_2}{I_1 N + 1} \quad \text{S8}$$

$$k_3 = \frac{N Z_2 S_1}{I_1 N + 1} \quad \text{S9}$$

where $I_1$ and $S_1$ are respectively the intercept and slope of the plot of $I_d/I_r$ *vs.* $\omega^{-1/2}$, and $S_2$ is the slope of the plot of $I_{dl}/(I_{dl}-I_d)$ *vs.* $\omega^{-1/2}$.

### 1.8 DFT Calculation

For better understanding of the mechanism underlying observed catalytic selectivity of Co-$N_4$/C towards ORR against HPRR, the reaction energies and Gibbs free reaction energies for ORR and HPRR reduction on Co-$N_4$ active sites in neutral media at equilibrium potential (U = 0 V) were calculated with density functional theory (DFT). The spin polarization DFT calculations were performed by the *Dmol*[3] module in *Materials Studio* 5.5 package, and generalized gradient approximation (GGA) with Perdew-Becke-Ernzerhof (PBE) was used for

the exchange-correlation functional. The double numerical plus polarization (DNP) basis set was used for the non-metal atoms. An accurate DFT Semi-core Pseudopots (DSPP) was employed for the Co atom. All of the models were calculated in periodically boxes with a vacuum slab of 15 Å to separate the interaction between periodic images. The simulated unite cell was hexagonal with $9.84 \times 9.84 \times 12.00$ Å$^3$. The energy, gradient and displacement convergence criterions were set as $1 \times 10^{-5}$ Ha, $2 \times 10^{-3}$ Å and $5 \times 10^{-3}$ Å, respectively. The free energy of the adsorbed state was calculated as:

$$\Delta G = \Delta E + \Delta E_{ZPE} - T\Delta S \quad \text{S10}$$

where $\Delta E$ is the reaction energy derived by DFT, $\Delta E_{ZPE}$ is the difference from the zero-point energy, and $T\Delta S$ is the change in entropy contribution to the free energy. The reactant adsorption step and the four and two electron pathways were used to simulate the ORR and HPRR processes, respectively shown in **Table S1**.

The chemical potential for the reaction ($H^+ + e^-$) is equal to that of 1/2 $H_2$ by setting the reference potential relative to the standard hydrogen electrode at standard neutral condition (pH = 0.0, $P_{H_2}$ = 1 bar, and $T$ = 298 K). ΔE, energy (i.e enthalpy) change; ΔG, free energy change at $T$ = 298 K, pH = 7.0 and U = 0 V.

### 1.9 *In vivo* experiments

Adult male Sprague-Dawley (SD) rats (300-350 g) were purchased from Beijing Vital River Laboratory Animal Technology Co., Ltd. (Beijing, China). A 12:12 h light-dark schedule was provided for the animals to live with food and water ad libitum, and animal experiments were performed with the method described previously.[4] Briefly, the animals were anaesthetized with isoflurane (4% induction, 2% maintenance) through a gas pump (RWD R520, Shenzhen, China) and positioned onto a stereotaxic frame. The working electrodes were carefully implanted into the rat brain and located at right cortex (A/P = -4.2 mm, M/L = -2.5 mm from bregma, D/V = -1.0 mm form dura) for *in vivo* $O_2$ monitoring. All animal procedures were approved and directed by the Institutional Animal Care and Use Committee of National Center for Nanoscience and Technology of China.

To study the hippocampal $O_2$ dynamics in pathological process, the rat was subjected to 2-VO global cerebral ischemia during *in vivo* real-time electrochemical sensing. The 2-VO ischemia process was constructed with ligation of the bilateral common carotids arteries (CCAs) with a 3-0 suture to induce temporary forebrain ischemia with the methods reported previously.[4]

### 1.10 Laser speckle flowmetry measurements

Laser speckle flowmetry (LSF) measurements were carried out with a noninvasive laser speckle imager (PeriCam PSI System, Perimed, Sweden).[6-9] Briefly, a CCD camera was positioned above the rat head with a laser diode (785 nm) illuminating the operated skull surface to allow penetration of the laser in a diffuse manner through the exposed brain region. The region of interest contrast (ROI) is defined as the speckle contrast ratio of pixel intensity to the mean pixel intensity, which is used to measure CBF as it is sampled from the speckle visibility relative to the velocity of the light-scattering particles (blood). LSF photographs gather the laser speckle signal of a small craniotomy operation area (2 mm × 2 mm square) of brain cortex near electrochemical recording area to obtain a real-time oxygen concentration change as indicated by the plot of ROI over time. Laser speckle perfusion images were obtained before 2-VO, during ischemia, and after reperfusion. ROI signals were recorded over time at 0.5 Hz by CCD camera and expressed as a normalized level of $O_2$ responses.

## 2. Supplementary Figures

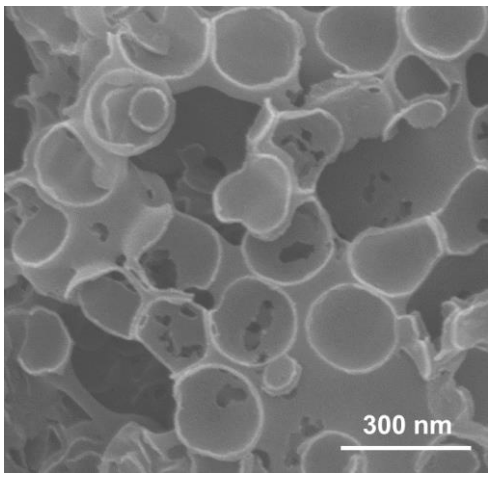


**Figure S1.** SEM image of the hollow spherical Co-$N_4$/C nanoparticles.

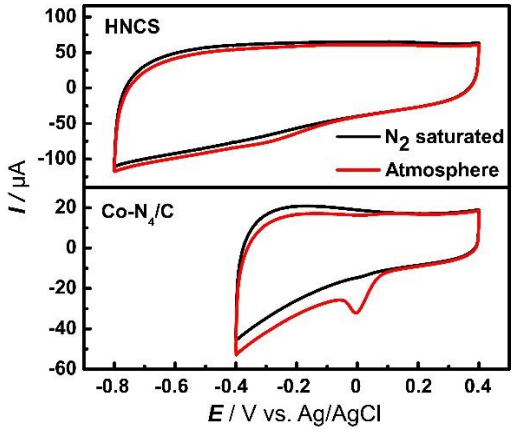


**Figure S2.** Typical cyclic voltammograms (CVs) obtained at metal-free HNCS-modified (up) and Co-$N_4$/C-modified (bottom) GCEs in phosphate buffer (pH 7.4) saturated with nitrogen or ambient air. Scan rate, 50 $mV \cdot s^{-1}$.

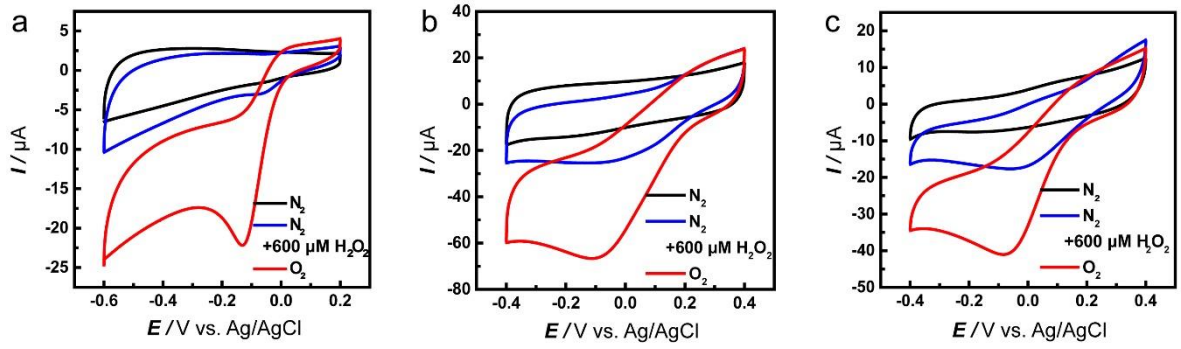


**Figure S3.** Typical CVs obtained at GCEs modified with Co-$N_4$/C (a), Pt/C (20%) (b) and electrodeposited Pt (c) in phosphate buffer (pH 7.4) saturated with $N_2$ in the absence (black line) or presence of 600 μm $H_2O_2$ (blue line) or saturated with $O_2$. Electrode surface loading densities of Co-$N_4$/C or Pt/C (20%) were 120 $\mu g \cdot cm^{-2}$. For Pt-GCE, Pt was electroplated on GCE. Scan rate, 50 $mV \cdot s^{-1}$

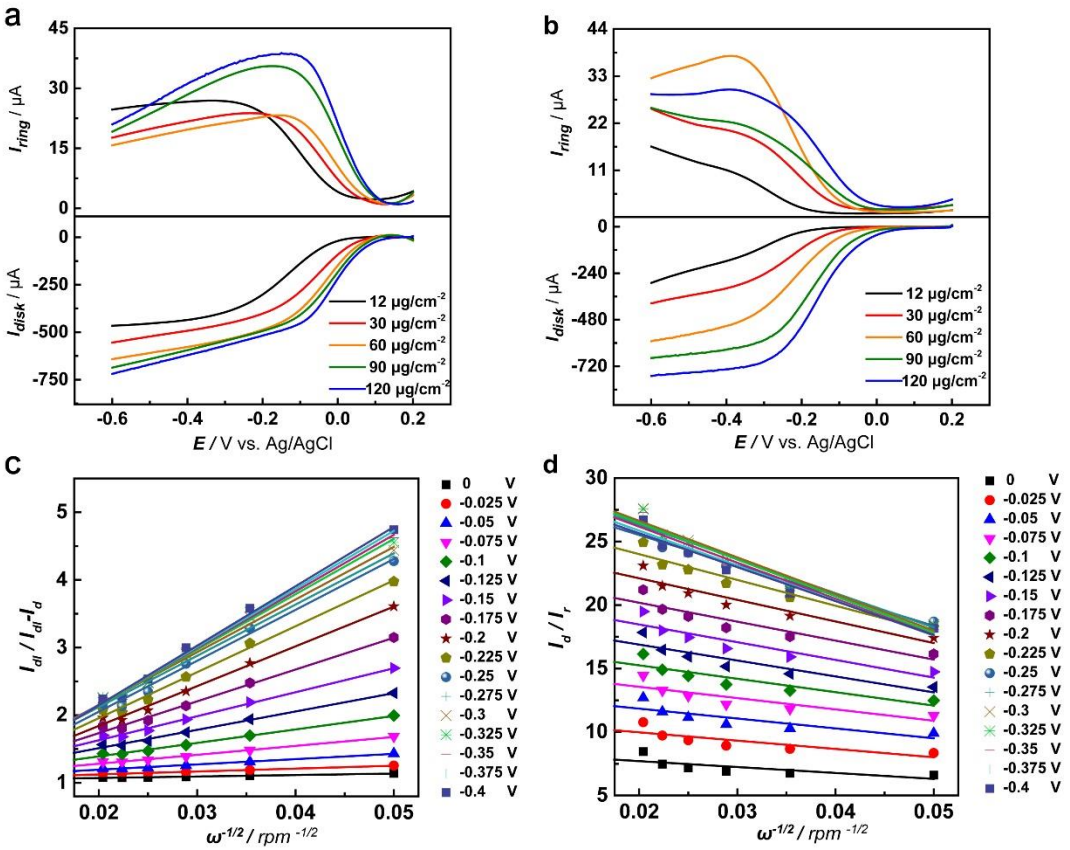


**Figure S4.** (a) (b) Typical RRDE curves obtained at Co-$N_4$/C-modified (a) and metal-free HNCS-modified (b) GC disk-Pt ring electrodes in $O_2$-saturated phosphate buffer (pH 7.4). The loading densities of Co-$N_4$/C and HNCS were 12, 30, 60, 90, and 120 μg·cm$^{-2}$. The bottom panels present the disk currents of ORR, and the upper panels present Pt ring currents of $H_2O_2$ oxidation at +0.50 V *vs*. Ag/AgCl. Scan rate: 5 mV·s$^{-1}$. Rotation speed: 1600 rpm. (c) (d) Typical plots of $I_d$ /$I_r$ *vs*. $\omega^{-1/2}$ (c) and plots of $I_{dl}$ /($I_{dl}$-$I_d$) *vs*. $\omega^{-1/2}$ (d) derived from Damjanovic simulation of ORR catalyzed by Co-$N_4$/C. Loading density of catalyst was 120 μg·cm$^{-2}$. Disk limiting current was obtained at 1600 rpm.

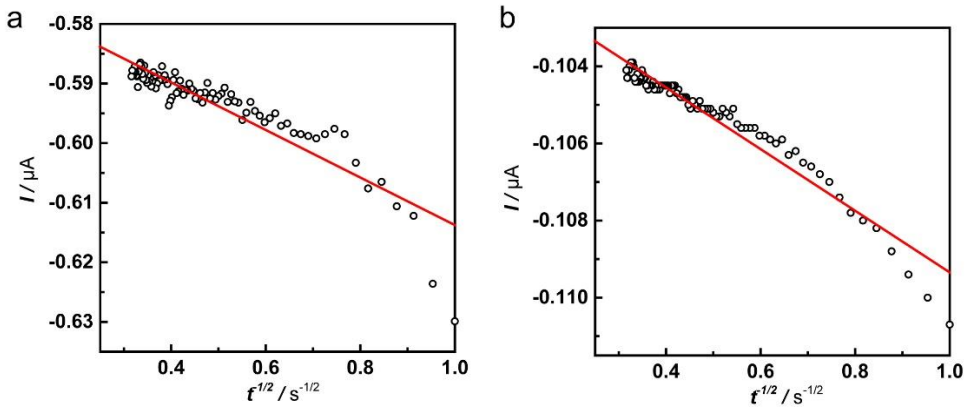


**Figure S5.** (a) ORR current *i vs*. $t^{-1/2}$ in a short period of time (0~10 s). (b) Potassium ferricyanide reduction current *i vs*. $t^{-1/2}$ in a short period of time (0~10 s). Measurements were conducted in phosphate buffer (pH 7.4). The red lines in (a) and (b) represent the linear-fitting lines of scattered data points. In this typical calculation, $I_{lim,ORR}$ = -5.90×10$^{-7}$ A, $c_O$ = 1.14 mM, $S_O$ = -3.99×10$^{-8}$ A·s$^{-1/2}$, $I_{lim\ FerriRR}$ = -1.02×10$^{-7}$A, $c_F$ = 1 mM and $S_F$ = -7.99×10$^{-9}$ A·s$^{-1/2}$. According to equation 1 and 2, the electron transfer number was calculated to be 3.78.

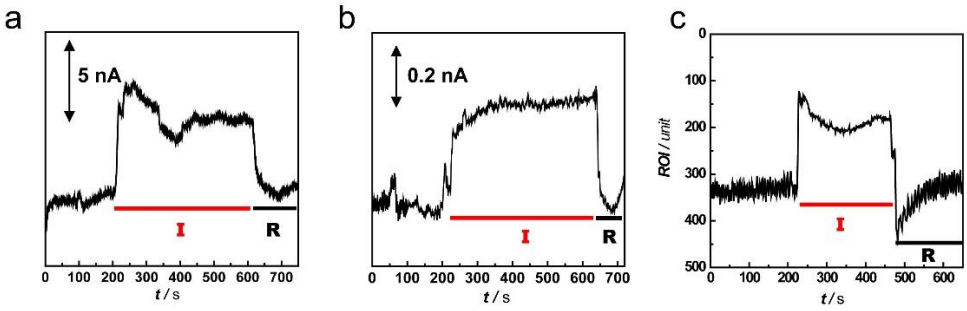


**Figure S6.** *In vivo* $O_2$ sensing. (a) (b) Typical amperometric current profile recorded by Co-$N_4$/C-CFE (a) or Pt-CFE (b) implanted in rat cortex over time during the 2-VO ischemia (I) and reperfusion (R) process. The sensing probe was polarized at -0.10 V *vs*. Ag/AgCl. Ischemia operations start at 200 s and reperfusions are implemented at approximately 600 s. (c) *In vivo* LSF recording of cortical $O_2$ fluctuation in the site of electrode implanted over time during the 2-VO ischemia and reperfusion process. Ischemia operations start at 200 s and reperfusions are implemented at approximately 500 s.

## 3. Supplementary Table

**Table S1**: Elementary steps of ORR and HPRR on Co-$N_4$/C with respective calculated reaction energies and Gibbs free energies.

| Elementary reactions | | $D_E$ (eV) | $D_G$ (eV) |
|---|---|---|---|
| ORR | $O_2(g) + * \rightarrow O_2*$ | -0.79 | -0.27 |
| | $O_2* + H^+ + e^- \rightarrow OOH*$ | -0.73 | -0.38 |
| | $OOH* + H^+ + e^- \rightarrow O* + H_2O$ | -0.63 | -0.86 |
| | $O* + H^+ + e^- \rightarrow OH*$ | -2.29 | -1.92 |
| | $OH* + H^+ + e^- \rightarrow H_2O$ | -0.45 | -0.70 |
| HPRR | $H_2O_2 + * \rightarrow H_2O_2*$ | -0.38 | 0.10 |
| | $H_2O_2* + H^+ + e^- \rightarrow OH* + H_2O$ | -2.65 | -2.78 |
| | $OH* + H^+ + e^- \rightarrow H_2O$ | -0.49 | -0.70 |

According to $D_G$ values obtained in **Table S1**, for HPRR, the initial adsorption step to form $H_2O_2$* is endothermic with $\Delta G = 0.10$ eV at $U = 0$, indicating that $H_2O_2$ activation is energetically blocked at the Co-$N_4$ sites due to weak peroxide-cobalt adsorbing interaction in the first place. This theoretically explains the $H_2O_2$ tolerance of Co-$N_4$/C catalyst.

## 4. References


(1) Stöber, W.; Fink, A.; Bohn, E., Controlled growth of monodisperse silica spheres in the micron size range. *J. Colloid Interface Sci.* **1968,** *26*, 62-69.

(2) Mayoral, R.; Requena, J.; Moya, J. S.; Lbpez, C.; Cintas, A.; Miguez, H., 3D long-range ordering in an $SiO_2$ submicrometer-sphere sintered superstructure. *Adv. Mater.* **1997,** *9*, 257-260.

(3) Han, Y.; Wang, Y. G.; Chen, W.; Xu, R.; Zheng, L.; Zhang, J.; Luo, J.; Shen, R. A.; Zhu, Y.; Cheong, W. C.; Chen, C.; Peng, Q.; Wang, D.; Li, Y., Hollow N-doped carbon spheres with isolated cobalt single atomic sites: superior electrocatalysts for oxygen reduction. *J. Am. Chem. Soc.* **2017,** *139*, 17269-17272.

(4) Xiang, L.; Yu, P.; Zhang, M.; Hao, J.; Wang, Y.; Zhu, L.; Dai, L.; Mao, L., Platinized aligned carbon nanotube-sheathed carbon fiber microelectrodes for in vivo amperometric monitoring of oxygen. *Anal. Chem.* **2014,** *86*, 5017-5023.

(5) Damjanovic, A.; Genshaw, M. A.; Bockris, J. O. M., Distinction between intermediates produced in main and side electrodic reactions. *J. Chem. Phys.* **1966,** *45*, 4057-4059.

(6) Jones, P. B.; Shin, H. K.; Boas, D. A.; Hyman, B. T.; Moskowitz, M. A.; Ayata, C.; Dunn, A. K., Simultaneous multispectral reflectance imaging and laser speckle flowmetry of cerebral blood flow and oxygen metabolism in focal cerebral ischemia. *J. Biomed. Opt.* **2008,** *13*, 044007.

(7) Shin, H. K.; Nishimura, M.; Jones, P. B.; Ay, H.; Boas, D. A.; Moskowitz, M. A.; Ayata, C., Mild induced hypertension improves blood flow and oxygen metabolism in transient focal cerebral ischemia. *Stroke* **2008,** *39*, 1548-55.

(8) Sakadžić, S.; Yuan, S.; Dilekoz, E.; Ruvinskaya, S.; Vinogradov, S. A.; Ayata, C.; A., B. D., Simultaneous imaging of cerebral partial pressure of oxygen and blood flow during functional activation and cortical spreading depression. *Appl. Opt.* **2009,** *48*, 169-177.

(9) Shang, Y.; Chen, L.; Toborek, M.; Yu, G., Diffuse optical monitoring of repeated cerebral ischemia in mice. *Opt. Express* **2011,** *19*, 20301-20315.